Proceedings of the
International Conference on Mechanical Engineering 2009
(ICME2009) 26- 28 December 2009, Dhaka, Bangladesh

ICME09-RT-05

INVESTGATION OF STRUCTURAL AND MAGNETIC PROPERTIES OF $Co_{1-x}Zn_xFe_2O_4$ PREPARED BY COMBUSTION TECHNIQUE

M. H. R. Khan[1], Farhad Alam[2], M. N. I. Khan[3], M.A. Hakim[3], D.K. Saha[3], and A. K. M. Akther Hossain[4]

[1]Department of Arts & Sciences, Ahsanullah University of Science & Technology, Dhaka, Bangladesh
[2]School of Engineering and Computer Science, Independent University, Bangladesh, Dhaka, Bangladesh.
[3]Materials Science Division, Atomic Energy Centre, Dhaka, Bangladesh
[4]Department of Physics, Bangladesh University of Engineering & Technology, Dhaka, Bangladesh

ABSTRACT

A series of polycrystalline $Co_{1-x}Zn_xFe_2O_4$ (x = 0, 0.1, 0.2 and 0.3) ferrites powders were prepared by combustion technique. Obtained fine nano-sized powders were calcined at low temperature (~973K). From the fine calcined powders, toroid and disk-shaped samples were prepared and sintered at various temperatures (1473K, 1523K and 1573K) in air for 5 hours. The bulk density and porosity of sintered samples were measured by Archimedes principle. The x-ray diffraction analysis confirmed that the samples are single-phase cubic spinel structure. The lattice parameter increases with increasing *Zn* content. This is due to the effect of ionic radii. Microstructural studies were carried out by high-resolution optical microscope. It is observed that grain size increases with increasing *Zn* content. The magnetic properties of these ferrites were studied in the frequency range 100Hz to 100MHz. It was observed that initial permeability increases with increasing sintering temperature up to 1523K and above 1523K permeability decreases. The experimental density, porosity, quality factor, and temperature dependent permeability of $Co_{1-x}Zn_xFe_2O_4$ are also investigated. The aim of these studies is to synthesize new materials with enhanced magnetic permeability for the creation of new technology.

Key words: Cubic spinel, Grain Size, Permeability, Ferrimagnet.

1. INTRODUCTION

Ferrites are extensively studied because of several interesting properties. They have spinel type crystal structure. It has tetrahedral *A*-site and octahedral *B*-sites in AB_2O_4 crystal structure. Depending on A-sites and B-sites cations they exhibit ferromagnetic, antiferromagnetic, spin (cluster) glass, and paramagnetic behaviour [1-6]. Polycrystalline spinel ferrites are widely used in many electronic devices. These are preferred because of their high permeability in the radio- frequency (RF) region, high electrical resistivity, mechanical hardness and chemical stability. These types of ferrites are subjects of intense theoretical and experimental investigation due to their remarkable magnetic and electric properties [7-9].

The *Co-Zn* ferrites are quite important in the field of microwave industry [10]. The $ZnFe_2O_4$ is normal spinel ferrites, while $CoFe_2O_4$ is inverse spinel; therefore, *Co-Zn* ferrite is mixed spinel type with interesting properties. Many efforts have been made to improve the basic properties of these ferrites by substituting or adding various cations of different valence states depending on the applications of interest [11-13]. In our present research we are interested to investigate the effect of substitution of divalent *Zn* in *Co* site on structural and magnetic properties of $Co_{1-x}Zn_xFe_2O_4$.

2. EXPERIMENTAL

The powders of $Co_{1-x}Zn_xFe_2O_4$ with (x = 0-0.3) were prepared through auto combustion method. The stoichiometric amounts of $Co(NO_3)_2.6H_2O$, $Zn(NO_3)_2.6H_2O$, $Fe(NO_3)_3.9H_2O$ were dissolved in ethanol. Then the solution was heated at a constant temperature bath (343K) to transform into gel, the dried gel burnt out to form fluffy loose powders. The resultant powders were calcined at 973K for 5h and then pressed uniaxially into disk-shaped (about 0.01 m outer diameter, 0.02-0.03 m thickness) and toroid-shaped (about 0.01 m outer diameters, 0.005 m inner diameter, and .003 m thickness) samples. The samples were sintered at 1473K, 1523K and 1573K for 5 h in air. The temperature ramps were $0.16Ks^{-1}$ for heating and $0.08Ks^{-1}$ for cooling. Microstructural properties were investigated with a high-resolution optical microscope. The bulk density was measured by $\rho_B = M/V$, where M is the mass of the sample and V is the volume. Average grain sizes (grain diameter) of the samples were determined from optical micrographs by linear intercept technique [14]. The

frequency dependent initial permeability of $Co_{1-x}Zn_xFe_2O_4$ was investigated using an Agilent Impedance Analyzer (Model no. 4192A). The complex permeability measurements on toroid-shaped samples have been carried out at room temperature in the frequency range 100Hz-100MHz. The values of the real part of the initial complex permeability (μ_i') have been calculated using the following relations: $\mu_i' = L_s/L_o$, where L_s is the self inductance of the sample core and $L_o = (\mu_o N^2 h/2\pi) ln(r_o/r_i)$ is derived geometrically, where L_o is the inductance of the winding coil without the sample core, N is the number of turns of the coil ($N = 5$), h is the thickness, r_o is the outer radius and r_i is the inner radius of the toroid-shaped sample. The relative quality factor (or Q factor) was calculated from the relation: $Q = \mu_i'/tan\delta$, where tanδ is the loss factor.

3. RESULTS AND DISCUSSION

3.1 Structural and Surface Morphology

The x-ray diffraction (XRD) patterns for the polycrystalline $Co_{1-x}Zn_xFe_2O_4$ compositions are presented in figure 1. The XRD peaks can be indexed to (111), (220), (311), (222), (400), (422), (511), (440) planes of spinel structure. The XRD patterns for these compositions confirm the formation of cubic spinel ferrites having no significant impurity. From XRD pattern the lattice parameters have been calculated with the help of Nelson-Riley function [2]. The lattice parameters of $Co_{1-x}Zn_xFe_2O_4$ compositions are plotted as a function of *Zn* content, as shown in figure 2a. The measured lattice parameter *'a'*, bulk density *'ρ_B'* and porosity *'P'* for different samples sintered at different temperatures are given in table 1. It is observed from the figure 2a that the variation of *'a'* with *Zn* contents in the $Co_{1-x}Zn_xFe_2O_4$ obey Vegard's law in the whole composition range under present investigation. '*a*' increases with increasing *Zn* content for all compositions. The increase in '*a*' with increasing *Zn* content can be explained on the basis of the ionic radii. The ionic radii of the cations used in $Co_{1-x}Zn_xFe_2O_4$ are 0.074 nm (Zn^{2+}), 0.072 nm (Co^{2+}) and 0.069 nm (Fe^{3+}) [15,16]. Since the ionic radius of Co^{2+} is less than that of the Zn^{2+}, increase in lattice constant with the increase in *Zn* substitution is expected.

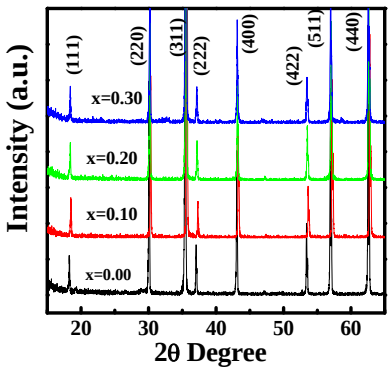

Fig 1. The x-ray diffraction pattern of polycrystalline $Co_{1-x}Zn_xFe_2O_4$.

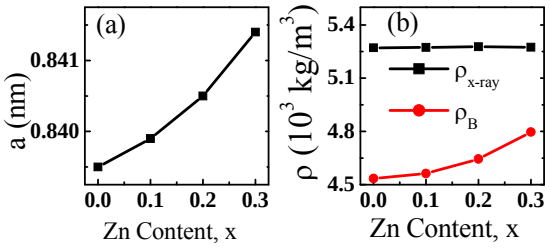

Fig 2. Variation of (a) lattice constants and (b) x-ray density and bulk density with Zn content of polycrystalline $Co_{1-x}Zn_xFe_2O_4$ sintered at 1473K.

The x-ray density $\rho_{x\text{-}ray}$ was calculated using following expression:

$$\rho_{x-ray} = \frac{8M_A}{N_A a^3}, \qquad (1)$$

where N_A is Avogadro's number (6.02×10^{23}), M_A is the molecular weight. The porosity was calculated from the relation, $P\,\% = \frac{\rho_{x-ray} - \rho_B}{\rho_{x-ray}} \times 100\,\%$, where ρ_B is the bulk density. The composition dependence $\rho_{x\text{-}ray}$ is shown in figure 2b. The ρ_B of the polycrystalline samples increases with increasing Zn content since the mass of Co^{2+} less than the mass of Zn^{2+}. Also ρ_B and P depends on sintering temperature, T_s. For different sintering temperatures such as 1473K, 1523K and 1573K, the ρ_B increases up to 1523K then decreases with further increasing sintering temperature. On the other hand, P of the sample decreases as increasing sintering temperature up to 1523K, and above 1523K the porosity increases as shown in the figure 3. This increase in density with increasing *Zn* content can be explained on

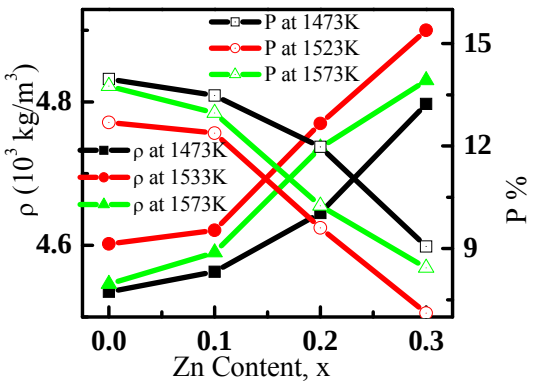

Fig 3. Variation of density and porosity as a function of Zn content for polycrystalline $Co_{1-x}Zn_xFe_2O_4$ sintered at different temperatures.

the basis of the atomic weight. It is observed that the porosity of ceramic samples originates from two sources, intragranular porosity and intergranular porosity. The total porosity could be written as $P = P_{intra} + P_{inter}$. The

intergranular porosity mainly depends on the grain size [9,17]. During the sintering process, the thermal energy generates a force that drives the grain boundaries to grow over pores, thereby decreasing the pore volume and densifying the samples.

Table 1: The lattice parameter, density, porosity and average grain size of $Co_{1-x}Zn_xFe_2O_4$ sintered at various temperatures, T_s, for 5 hours in air.

x	a (nm)	T_s (K)	$\rho_{x\text{-}ray}\ 10^3$ (kg/m^3)	$\rho_B\ 10^3$ (kg/m^3)	P (%)	μ_i'	Grain Size (μm)
0.0	0.8395	1473	5.271	4.54	14.0	26	1.57
		1523		4.60	12.7	27	2.10
		1573		4.55	13.7	25	2.96
0.1	0.8399	1473	5.274	4.56	13.5	31	1.84
		1523		4.62	12.4	34	2.45
		1573		4.59	12.9	28	3.10
0.2	0.8405	1473	5.277	4.65	11.9	33	2.06
		1523		4.77	9.60	38	2.98
		1573		4.74	10.3	30	3.56
0.3	0.8414	1473	5.275	4.80	9.10	38	2.45
		1523		4.90	7.10	40	3.12
		1573		4.83	8.40	36	3.86

At higher sintering temperatures the density decreases because of increasing intragranular porosity resulting from discontinuous grain growth. Such a conclusion is in agreement with that previously reported in case of *Ni-Zn* ferrites [9].

Figure 4 shows micrographs of various $Co_{1-x}Zn_xFe_2O_4$ samples sintered at different temperatures. Well-developed grains with fewer pores were observed for all samples. The grain size is found to increase with increasing *Zn* content and different sintering temperatures. The microstructure becomes more uniform and compact with increasing *Zn* content as a result intergranular pores disappear and grains become large. The average grain size for different sintering temperatures is presented in table 1.

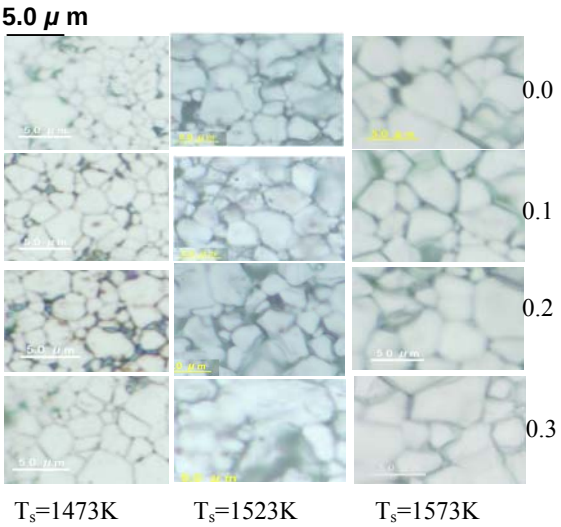

Fig 4. The optical micrographs of polycrystalline $Co_{1-x}Zn_xFe_2O_4$ (x=0.0-0.3) samples sintered at various temperatures.

3.2 Initial Permeability

Figure 5 shows the frequency dependent real part of initial permeability, μ_i', values of $Co_{1-x}Zn_xFe_2O_4$ sintered at 1523K. From this figure we observed that the μ_i' increases with increasing *Zn* content. Similar observation is observed at samples sintered at 1473K and 1573K. Figure 6 represents the frequency dependent μ_i' for $Co_{0.7}Zn_{0.3}Fe_2O_4$ sintered at different temperatures. It is observed that the μ_i' for all samples increase as the T_s increases up to 1523K and above 1523K it decreases. Therefore, μ_i' is related to the ρ_B, P and microstructure of the samples.

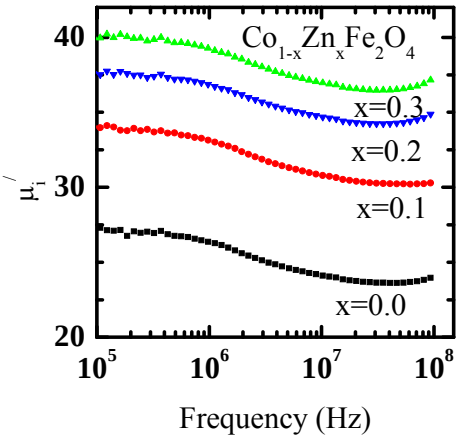

Fig 5. Real part of initial permeability of polycrystalline $Co_{1-x}Zn_xFe_2O_4$ samples sintered at 1523K.

It is well known that the magnetization process can be characterized as superposition of domain wall motion and spin rotation [12].

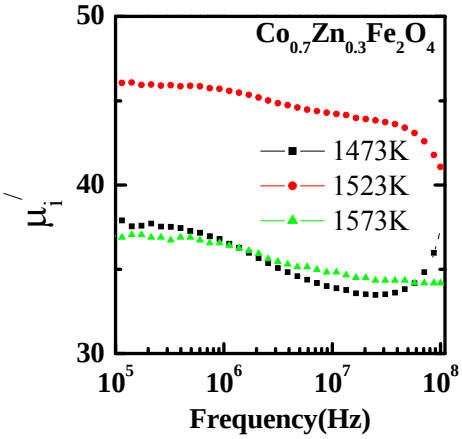

Fig 6. Real part of initial permeability of polycrystalline $Co_{0.7}Zn_{0.3}Fe_2O_4$ sample sintered at 1473K, 1523K and 1573K.

So, the permeability can be described as [5,6]

$$\mu_i' = 1 + \chi_{spin} + \chi_{dw}, \qquad (2)$$

where χ_{spin} and χ_{dw} denote the magnetic susceptibility of spin and domain wall motion, respectively. χ_{dw} and χ_{spin} can be written as: $\chi_{dw} = 3\pi M_s^2 D/4\gamma$ and $\chi_{spin} = 2\pi M_s^2/K$,

where M_s, K, D and γ are the saturation magnetization, total anisotropy energy, average grain diameter and domain wall energy, respectively [18]. Since the magnetic anisotropy field $H_A = 2K/M_s$, χ_{spin} can be represented by, $\chi_{spin} = 4\pi Ms/H_A$ [19].

For polycrystalline ferrites, pores and other imperfections are unavoidable, which generate a demagnetizing field. So, anisotropy field consists of magnetic anisotropy field H_A and demagnetizing field H_d. Therefore, χ_{spin} should be represented by $\chi_{spin} = 4\pi Ms/(H_A + H_d)$. In our present investigation H_d decreases because pores decrease and grains become bigger with increasing *Zn* content consequently χ_{spin} increases. The sample doped with *Zn* content possesses the most compact and uniform microstructure in all samples. The grain size increases with *Zn* content and therefore the increasing permeability with *Zn* content could be attributed to grain size. Our results agree with the results reported by Yan, M *et.al.* [19] and Karche, B. R. *et.al.* [20] in *Ni-Cu-Zn* and *Mg-Cd* ferrites.

From the figure 5, it is observed that the resonance peaks are beyond 100MHz. This indicates that these materials are useful for fabrication of devices up to 100MHz.

From the observed loss factor we have calculated the Q factor for the polycrystalline $Co_{1-x}Zn_xFe_2O_4$ compositions sintered at various sintering temperatures. The Q factors at 1523K are shown in figure 7. It is observed that Q factor increases with increasing Zn content. The highest Q factor is observed for $Co_{0.7}Zn_{0.3}Fe_2O_4$ sintered at 1523K.

3.3 Temperature Dependent Initial Permeability

The variation of μ_i' with temperature for various $Co_{1-x}Zn_xFe_2O_4$ samples sintered at 1473 K is shown in figure 8. The temperature dependent μ_i' of the samples is measured

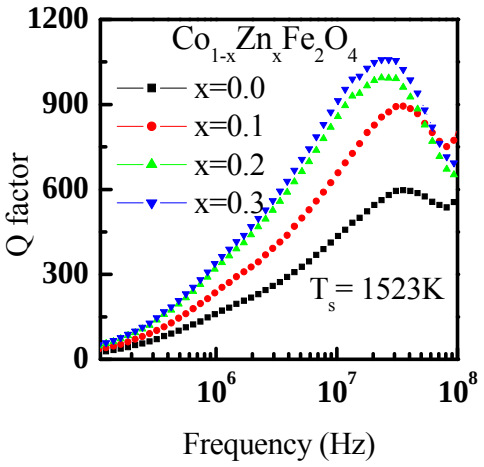

Fig 7. The Q factor of polycrystalline $Co_{1-x}Zn_xFe_2O_4$ sintered at 1523K.

at an arbitrary constant frequency (100 kHz).The μ_i' slowly increases with temperature, reaches a maximum and then sharply drops to lower value at certain temperature. This temperature is called Néel temperature, T_N. The increase μ_i' with temperature can be explained as follows: The anisotropy field usually decreases with temperature much faster than M_s [4, 21]. The intrinsic parameters of the sample that affect μ_i' are saturation magnetization and magnetocrystaline anisotropy. It is also dependent upon the degree of wall continuity across the grain boundaries as shown by Globus *et.al* [22]. Since saturation magnetization and anisotropy constant vary with temperature, μ_i' is a complicated function of temperature and it is difficult to derive any qualitative inference.

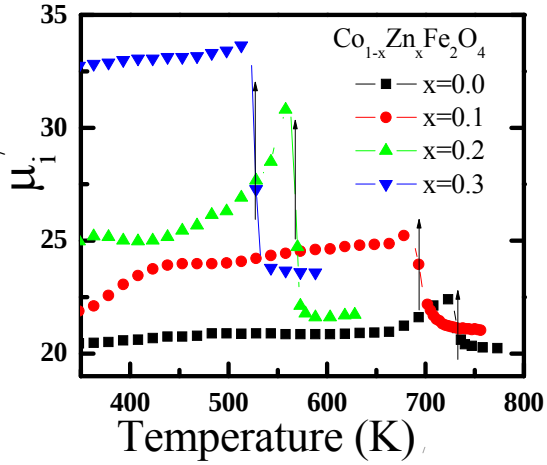

Fig 8. The initial permeability as a function of temperature for $Co_{1-x}Zn_xFe_2O_4$ samples sintered at 1473K.

From the figure 8 we observed that μ_i'-T curves suddenly drop to lower value at T_N. The T_N values decrease continuously with *Zn* content due to weakening of the A-B interaction on additions of non-magnetic Zn content. Similar observation has been reported in the case of *Zn* substituted *Ni-Cu* and *Li-Cu* ferrites [23,24].

4. CONCLUSION

Phase pure $Co_{1-x}Zn_xFe_2O_4$ ferrites are prepared by combustion method. The XRD pattern confirms that all the samples exhibit cubic spinel structure. The μ_i' values are strongly depend on the density, sintering temperature and microstructures of the samples. Ferrimagnetic to paramagnetic transition is observed in all the samples. Substitution of *Zn* increases permeability values but lowers the Néel temperature. The appropriate amount of *Zn* substitution helps to improve the magnetic properties of these ferrites.

5. REFERENCES

1. Tsutaoka, T., 2003 "Frequency dispersion of complex permeability in Mn–Zn and Ni–Zn spinel ferrites and their composite materials" J. Appl. Phys., Vol. 93, No. 5.
2. Akther Hossain, A. K. M, Seki, M., Kawai, T., and Tabata, H., 2004 "Colossal magnetoresistance in spinel type $Zn_{1-x}Ni_xFe_2O_4$," *J. Appl. Phys.*, **96**, 1273.

3. Snoek, J. S., 1949, *New Developments in Ferromagnetic Materials,* Elsevier Publishing Company, Inc., New York.
4. Valenzuela, R., 1994, *Magnetic Ceramics*, Cambridge University Press, Cambridge.
5. Ahmed, M. A., Okasa, N. and Salah, L., 2003, "Influence of yttrium ions on the magnetic properties of Ni-Zn ferrites," J. Magn. Magn. Mater. 264: 241.
6. Verma, A., Goel, T. C., Mendiratta and Kishan, P., 2000, "Magnetic properties of nickel-zinc ferrites prepared by the citrate precursor method," J. Magn. Magn. Mater., 208: 13.
7. El-Shabasy, M., 1997, "DC electrical properties of Ni-Zn ferrites," J. Magn. Magn. Mater., 172:188.
8. Rosales, M. I., Amano, E., Cuautle, M. P. and Valenzuela, R., 1997, "Impedance spectroscopy studies of Ni-Zn ferrites," Materials Science and Engineering, B 49: 221.
9. Mahmud, S.T., Akther Hossain, A.K.M., Abdul Hakim, A.K.M., Seki, M., Kawai, T. and Tabata, H., 2006, "Influence of microstructure on the complex permeability of spinel type Ni–Zn ferrite" J. Magn. Magn. Mater., 305 : 269–274.
10. Josyulu, O.S., Sobhanadri and Viswanatham, B., 1981, Rev. Roum. Chim. 26(5):687.
11. Shukla, S.J., Jadhav, K.M. and Bichile, G.K., 1999, "Influence of Mg substitution on magnetic properties of Co-Fe-Cr-O spinel ferrite system" J. Magn. Magn. Mater., 195: 692-698.
12. Arulmurugan, R., Jeyadevan, B., Vaidyanathan, G. and Sendhilnathan, S., 2005, "Effect of zinc substitution on Co–Zn and Mn–Zn ferrite nanoparticles prepared by co-precipitation" J. Magn. Magn. Mater., 288 : 470–477.
13. Brabers, V.A.M., 1995, *Handbook of Magnetic Materials,* ed. By. K. H. Buschow (Elsevier Science B.V.) Vol. 8, p 189.
14. Verma, A., Goel, T. C., Mendiratta, R. G. and Kishan, P., 2000, "Magnetic properties of nickel-zinc ferrites prepared by the citrate precursor method," J. Magn. Magn. Mater., 208:13.
15. James E. Huhecy, *Inorganic Chemistry (Principles of structure and Reactivity),* Fourth edition.
16. Shannon, R.D., 1976, *Acta Crystallogr.* A 32: 751.
17. Sattar, A. A., El-Sayed, H. M., El-Shokrofy, K. M. and El-Tabey, M. M., 2005, "Improvement of the magnetic properties of Mn-Ni-Zn ferrite by the non-magnetic Al^{3+} ion substitution," J. Appl. Sci., 5(1):162.
18. Slick, P.I., 1980, *Ferromagnetic Materials, vol.2*, in: E.P. Wohlforth (Ed.), North-Holland, Amsterdam.
19. Yan, M., Hu, J., Luo, W. and Zhang, W.Y., 2006, "Preparation and investigation of low firing temperature NiCuZn ferrites with high relative initial permeability" J. Magn. Magn. Mater., 303 : 249–255.
20. Karche, B. R., Khasbardar, B. V. and Vaingankar, A.S., 1997, "X-ray, SEM and magnetic properties of Mg-Cd ferrites" J. Magn. Magn. Mater., 168: 292-298.
21. Cullity, B. D., 1972, *Introduction to Magnetic Materials*, Addison-Wesley Publishing Company, Inc., California.
22. Glubus, A. and Duplex, P., 1969, "Size of bloch wall and parameters of the magnetic susceptibility in ferrimagnetic spinels and garnets", Phys. Stat. Sol. A 31: 765
23. Ahmeda, M.A., and EL-Sayed, M.M., 2007, "Magnetic characterization and thermoelectric power of $Ni_{1-y}Zn_y\ Cu_{0.3}Fe_{1.7}\ O_4$" J. Magn. Magn. Mater., 308:40–45.
24. Jadhav, S. A., 2001, "Magnetic properties of Zn-substituted Li-Cu ferrites" J. Magn. Magn. Mater., 224: 167-172.

6. NOMENCLATURE

Symbol	Meaning	Unit
$\rho_{x\text{-}ray}$	X-ray density	(kg/m^3)
ρ_B	Bulk density	(kg/m^3)
$\mu_i^{/}$	Real part of initial permeability	Dimensionless
a	Lattice parameter	(nm)
P	Porosity	Dimensionless
Q	Relative quality factor	Dimensionless

7. MAILING ADDRESS

M. H. R. Khan
Department of Arts & Sciences,
Ahsanullah University of Science & Technology,
Dhaka, Bangladesh